# Supporting Information

## Dalebroux et al. 10.1073/pnas.1316901111

### SI Text

**Note S1.** The amount of outer membrane (OM) acyl-PG in $phoQ^{cHAMP}$ versus $phoQ^{T48I}$ was statistically identical for all species by liquid-chromatography and collision-induced-dissociation mass spectrometry (LC-MS/MS). Therefore, $phoQ^{cHAMP}$ was excluded from further analytical measurements for determining OM acyl-PG levels.

**Note S2.** To estimate the percent abundance of each glycerophospholipid (GPL) family within the OM, the absolute pg/μL value for one representative species from each family was divided by the sum of the total value for the four representative species. Because C16:0/C18:1 is a predominant acyl combination in GPL, phosphatidylethanolamine (PE) 16:0/18:1, *m/z* 716, phosphatidylglycerol (PG) 16:0/18:1, *m/z* 747, acyl-PG 16:0/18:1/14:0, *m/z* 955, and cardiolipin (CL) 16:0/18:1–16:0/18:1, *m/z* 1404, were selected for analysis (1–3). LC-MS/MS estimated the wild-type OM to be 75% PE, 15% PG, 9% acyl-PG, and 1% CL, values similar to those previously reported: 81.3% PE, 17.1% PG, and 1.6% CL; however, acyl-PG levels were not determined (4). During high activation of the PhoP/PhoQ response regulator/histidine kinase two-component system, PE remained static at 75% whereas acidic GPL changed dramatically, shifting to 9% PG, 12% acyl-PG, and 4% CL. Rough estimates predict that 60% of the total OM acyl-PG is palmitoylated when PhoPQ is activated.

### SI Materials and Methods

**Electrospray-Ionization Time-of-Flight Mass-Spectrometry.** Instrumental settings were as follows: cone voltage, 35 V; capillary voltage, 3.3 kV; extractor, 4; desolvation temperature, 350 °C; source temperature, 120 °C; and gas flow of nitrogen, 800 L/h. The time-of-flight (TOF) was calibrated before each use using sodium formate (NaF) over a mass range of 100–2,000 acquired in continuum mode with an acceptable tolerance of less than 2 ppm difference across the mass range. Leucine Enkephalin was used as a lock mass during acquisition to ensure proper mass assignment to analytes of interest. Mobile phase consisted of 5% Fisher Optima LC-MS grade water and 95% Fisher Optima LC-MS grade methanol. Collision induced dissociation (CID) or MS/MS analysis was also performed on the Waters Synapt TOF, using conditions described above, to determine the daughter ions of each compound of interest by increasing the collision energy to 30 kV. Each parent ion was isolated in the quadrupole region, and CID in the trap region of the system induced fragmentation.

**Normal-Phase LC-MS/MS.** Retention of PG, CL, and PE was achieved at a flow rate of 0.25 mL/min using mobile phase A [$CHCl_3$/$CH_3OH$/$NH_4OH$ (800:195:5, vol/vol/v)], and mobile phase B [$CHCl_3$/$CH_3OH$/$H_2O$/$NH_4OH$ (600:340:50:5, vol/vol/vol/vol). A three-step gradient used started at 0% B for 1 min, continued at 0–50% B over the next 3 min, was held at 50% B for 4 min, returned to starting conditions in 0.1 min, and was allowed to equilibrate for an additional 3 min, giving a total run time of ∼11 min. The following parent-to-daughter ion transitions were monitored [multiple reaction monitoring (MRM)]: 660.5 > 253.2 PE, 716.2 > 281.6 PE, 742.2 > 281.6 PE, 747.6 > 255.3 PG, 661.4 > 255.3 CL, 674.6 > 255.3 CL, 687.5 > 253.3 CL, 701.5 > 255.3 CL (1, 3). Each daughter ion monitored corresponded to a distinct fatty-acid fragment. Mass transitions were determined by CID and daughter ion monitoring (1, 3). In the case of PE and PG, singly charged $[M\text{-}H]^-$ parent > daughter ion transitions were monitored. For CL, doubly charged $[M\text{-}2H]^{2-}$ ions were monitored because they were more abundant than singly charged ions. Instrumental settings were as follows: cone voltage, 50–65 V depending on the target; collision energy, 35–40 V; capillary voltage, 3.3 kV; extractor, 4; desolvation temperature, 350 °C; source temperature, 120 °C; and gas flow of nitrogen, 800 L/h. To determine the retention time of PE, PG, and CL, pure standards (Avanti) were monitored. Standards included 1-palmitoyl-2-oleoyl-*sn*-glycero-3-phosphoethanolamine, C16:0–18:1 PE, *m/z* 716.7, 1-palmitoyl-2-oleoyl-*sn*-glycero-3-phospho-(1'-*rac*-glycerol), C16:0–18:1 PG, *m/z* 747.6, and 1',3'-bis[1,2-dioleoyl-*sn*-glycero-3-phospho]-*sn*-glycerol, C18:1 × 4 CL, *m/z* 1452.3. To survey GPL throughout the gradient, we scanned parent ions from an OM GPL extract of $phoQ^{cHAMP}$ mutant *S.* Typhimurium using the following instrumental settings: cone voltage, 30 V; capillary voltage, 3.3 kV; extractor, 4; desolvation temperature, 350 °C; source temperature, 120 °C; and gas flow of nitrogen, 800 L/h.

**Reversed-Phase LC-MS/MS of OM Extracts.** Retention of PG, acyl-PG, and PE was achieved at a flow rate of 0.3 mL/min using mobile phase A, consisting of water, and mobile phase B, consisting of $CH_3OH$. A three-step gradient used started at 50% B for 1 min, continued at 50–100% B over the next 6 min, was held at 100% B for 1 min, returned to starting conditions in 0.1 min, and was allowed to equilibrate for an additional 2 min, for a total run time of ∼10 min. Data were obtained using MRM and the following ion transitions: 660.5 > 253.2 PE, 716.2 > 281.6 PE, 742.2 > 281.6 PE, 747.6 > 255.3 PG, 929.8 > 253.2 acyl-phosphatidylglyerol (APG), 955.8 > 253.2 APG, 958.5 > 255.3 APG, 983.8 > 253.2 APG, 1009.5 > 281.6 APG, and 1012.8 > 281.6 APG (2, 3). Instrumental settings were as follows: cone voltage, 65 V; collision energy, 40 kV; capillary voltage, 3.5 kV; extractor, 4; desolvation temperature, 350 °C; source temperature, 120 °C; and gas flow of nitrogen, 800 L/h. To determine retention time of PE and PG and to generate standard curves for quantitative analysis, standards were monitored. Integrated peak areas were plotted against standard concentration to generate a linear equation to which the peak area values generated from specific PG, PE, and acyl-PG parent > daughter ion transitions were applied. Using our standard curve, we calculated the amount (ng) of the PE, PG, and acyl-PG per μL of sample. Because a commercial standard does not exist, acyl-PG retention was determined by parent ion scanning between *m/z* 920 and 1020 and by targeting parent > daughter ion transitions described previously (2). For acyl-PG quantification, we applied peak area values to the standard curve generated for the PG dilution series. We reasoned that, because their peak shapes were similar and instrument conditions were identical, the PG curve should adequately predict the amount of acyl-PG per μL of sample.

**LC-MS/MS of PagP-PG Reaction Products.** To increase separation and therefore resolution of the acyl-PG molecule, a Phenomenex Luna 5 μ phenyl-hexyl column (75 × 4.66 mm) was used. Glycerophospholipid retention was achieved at a flow rate of 0.3 mL/min using mobile phase A, consisting of water, and mobile phase B, consisting of $CH_3OH$. A three-step gradient used started at 75% B for 1 min, continued at 75–100% B over the next 5 min, was held at 100% B for 14 min, returned to starting conditions in 0.1 min, and was allowed to equilibrate for an additional 2 min for a total run time of ∼24 min. To survey GPL throughout the gradient, parent ions were scanned using the same instrumental settings described above for normal-phase LC-MS/MS. For

targeted analysis, CID and MRM were carried out as described for reversed-phase LC-MS/MS of OM extracts with the following exception. The parent-to-daughter ion transition monitored for the palmitoyl-PG product was $m/z$ 985.80 > 255.0.


1. Hsu FF, Turk J (2006) Characterization of cardiolipin from *Escherichia coli* by electrospray ionization with multiple stage quadrupole ion-trap mass spectrometric analysis of [M - 2H + Na]- ions. *J Am Soc Mass Spectrom* 17(3):420–429.
2. Hsu FF, Turk J, Shi Y, Groisman EA (2004) Characterization of acylphosphatidylglycerols from *Salmonella typhimurium* by tandem mass spectrometry with electrospray ionization. *J Am Soc Mass Spectrom* 15(1):1–11.
3. Oursel D, et al. (2007) Lipid composition of membranes of *Escherichia coli* by liquid chromatography/tandem mass spectrometry using negative electrospray ionization. *Rapid Commun Mass Spectrom* 21(11):1721–1728.
4. Osborn MJ, Gander JE, Parisi E, Carson J (1972) Mechanism of assembly of the outer membrane of *Salmonella typhimurium*. Isolation and characterization of cytoplasmic and outer membrane. *J Biol Chem* 247(12):3962–3972.


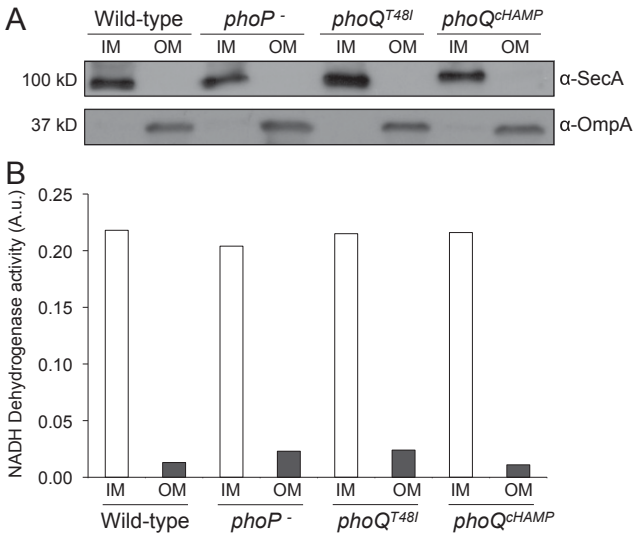


**Fig. S1.** (*A*) Western blots for the *S*. Typhimurium SecA and OmpA proteins to demonstrate purity of the IM and OM fractions, repectively. (*B*) NADH oxidation was monitored following addition of 5 μg of protein from membrane fractions and measuring the decrease in absorbance at 340 nM after 2 min of incubation at 22 °C. Graphed is the inverse of the change in absorbance of each sample relative to a no-enzyme control reaction. Representative experiments and arbitrary units (A.u.) are shown.

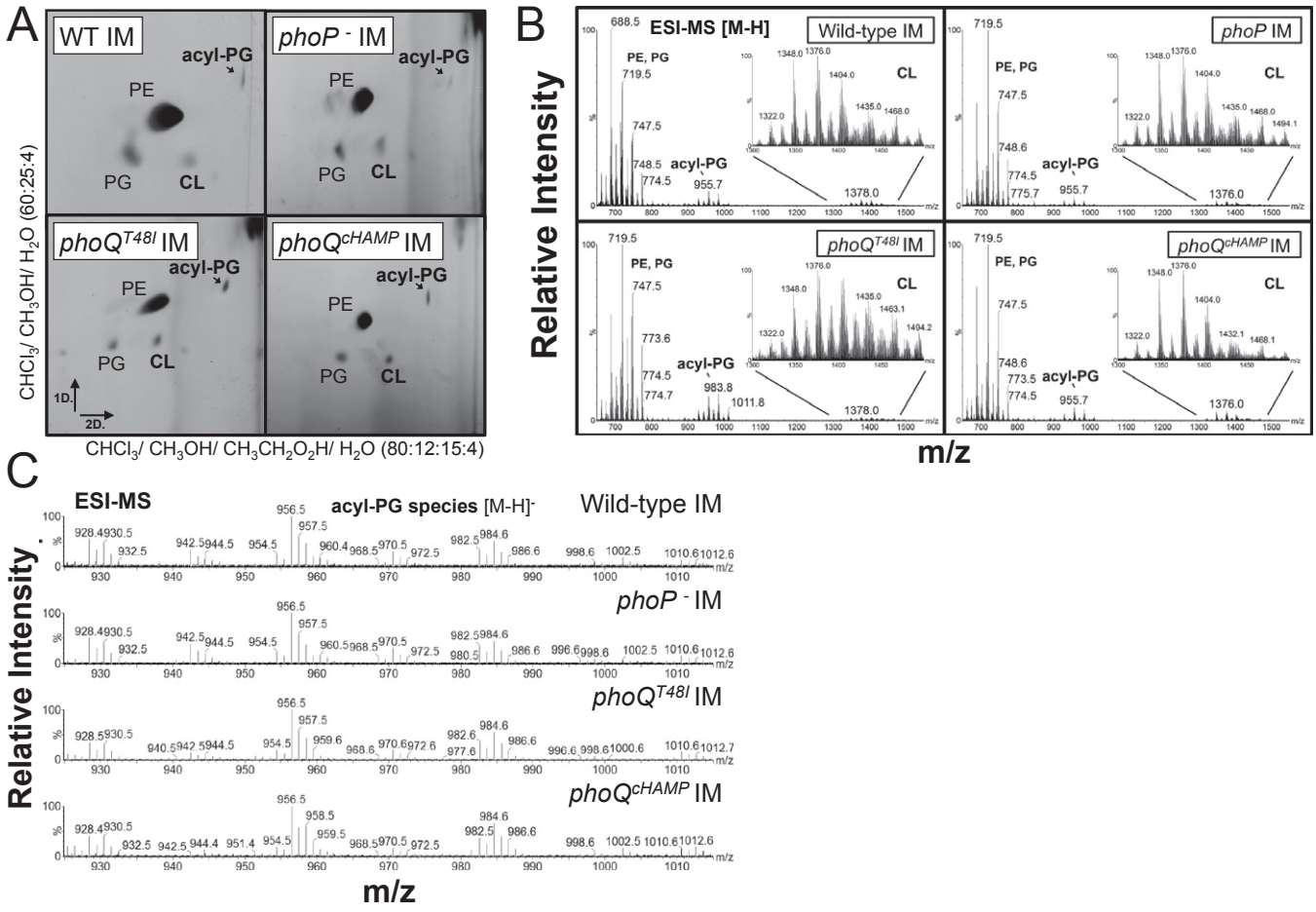


**Fig. S2.** Inner membrane (IM) GPLs were extracted and separated by (*A*) 2D TLC with the solvents specified, or (*B*) electrospray-ionization time-of-flight mass-spectrometry (ESI-MS). Shown are iodine stained TLC plates and mass spectra from one of several experiments. Relative intensity reflects the percent intensity of each peak relative to the highest peak in the *m/z* range depicted. (C) ESI-MS parent ion spectra of acyl-PG from GPL extracts collected from the IM of *S*. Typhimurium.

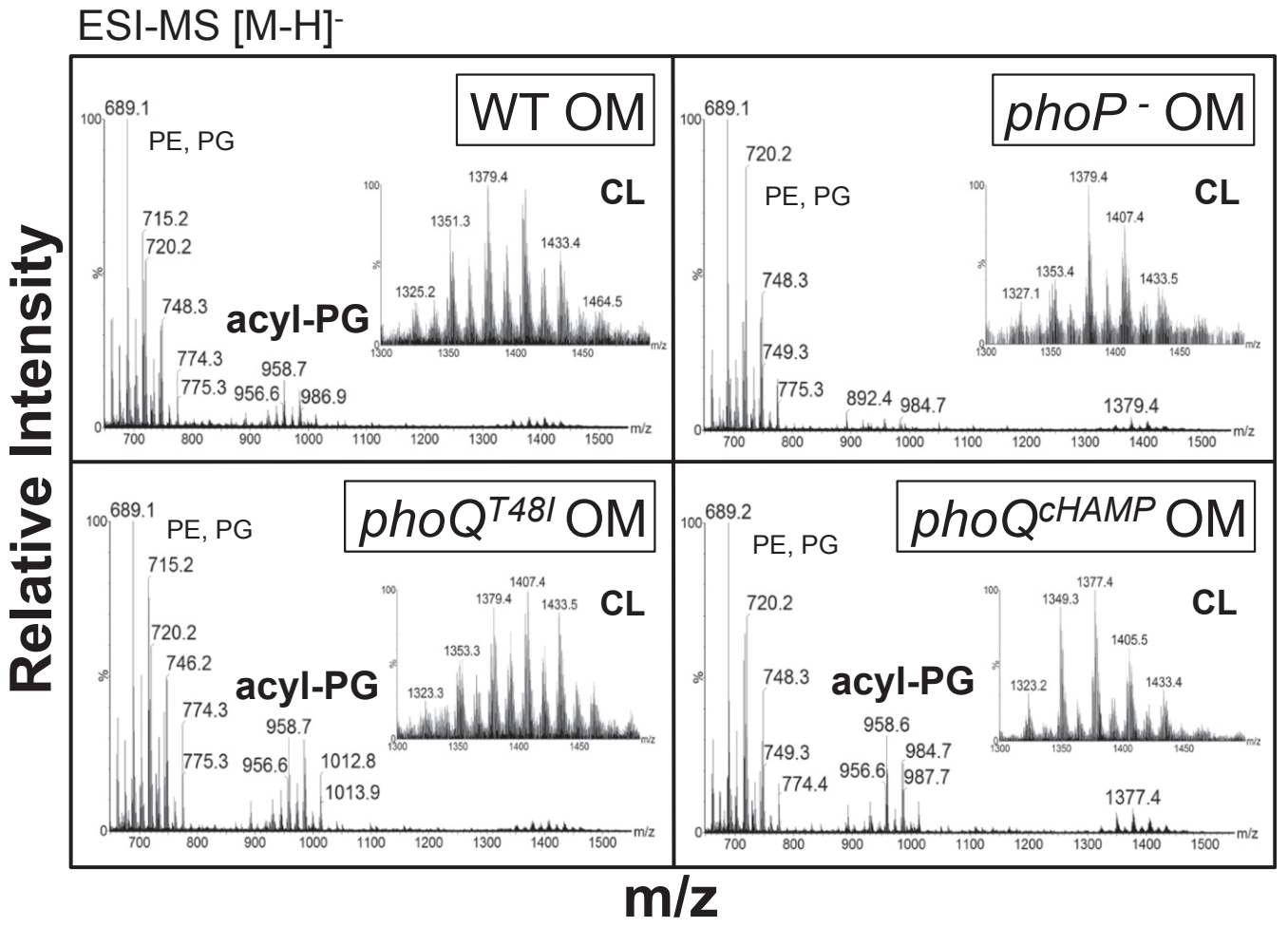


**Fig. S3.** ESI-MS of GPL collected from outer membranes (OM) of the bacterial strains indicated. Relative intensity reflects the intensity of each peak relative to the highest peak in the range.

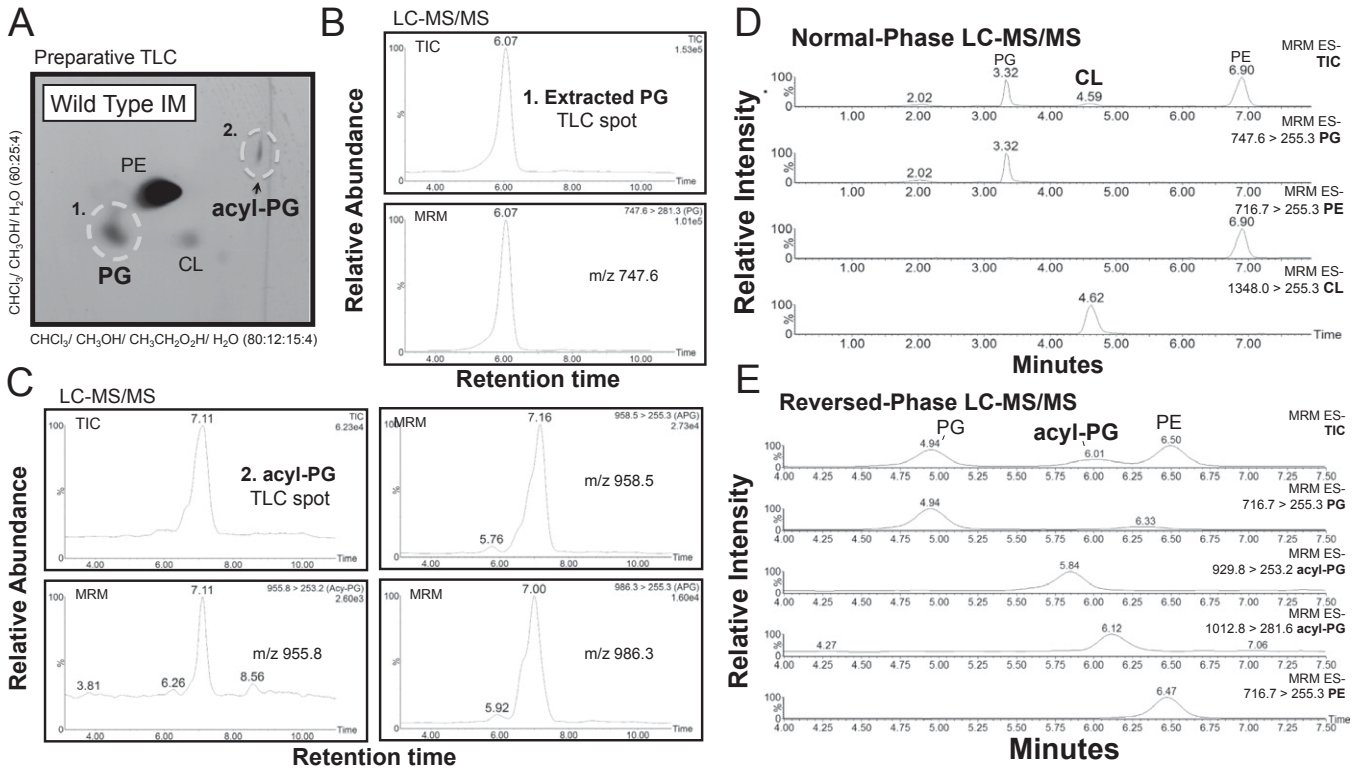


**Fig. S4.** To confirm the identity of the predicted acyl-PG spot, GPL were separated by (*A*) TLC. Spots corresponding to (*B*) PG and (*C*) acyl-PG were extracted and analyzed by LC-MS/MS. (*C*) Normal phase LC-MS/MS of *S*. Typhimurium OM GPL. The total ion current (TIC) chromatogram and parent-to-daughter ion transitions for three representative GPL are shown. Total ion current chromatograms reflect the sum of all transitions monitored. Daughter ions detected correspond to palmitic acid (*m/z* 255.3). Multiple reaction monitoring (MRM) refers to simultaneous monitoring of multiple parent-to-daughter ion transitions. (*D*) Normal-phase LC-MS/MS was used to separate and quantify *S*. Typhimurium CL. (*E*) Reversed-phase LC-MS/MS was used to separate and quantify *S*. Typhimurium acyl-PG. Depicted is the TIC chromatogram and parent-to-daughter ion transitions for four representative GPL. Daughter ions correspond to palmitoleic acid (C16:1) (*m/z* 253.2) and *cis*-vaccenic acid (C18:1) (*m/z* 281.6).

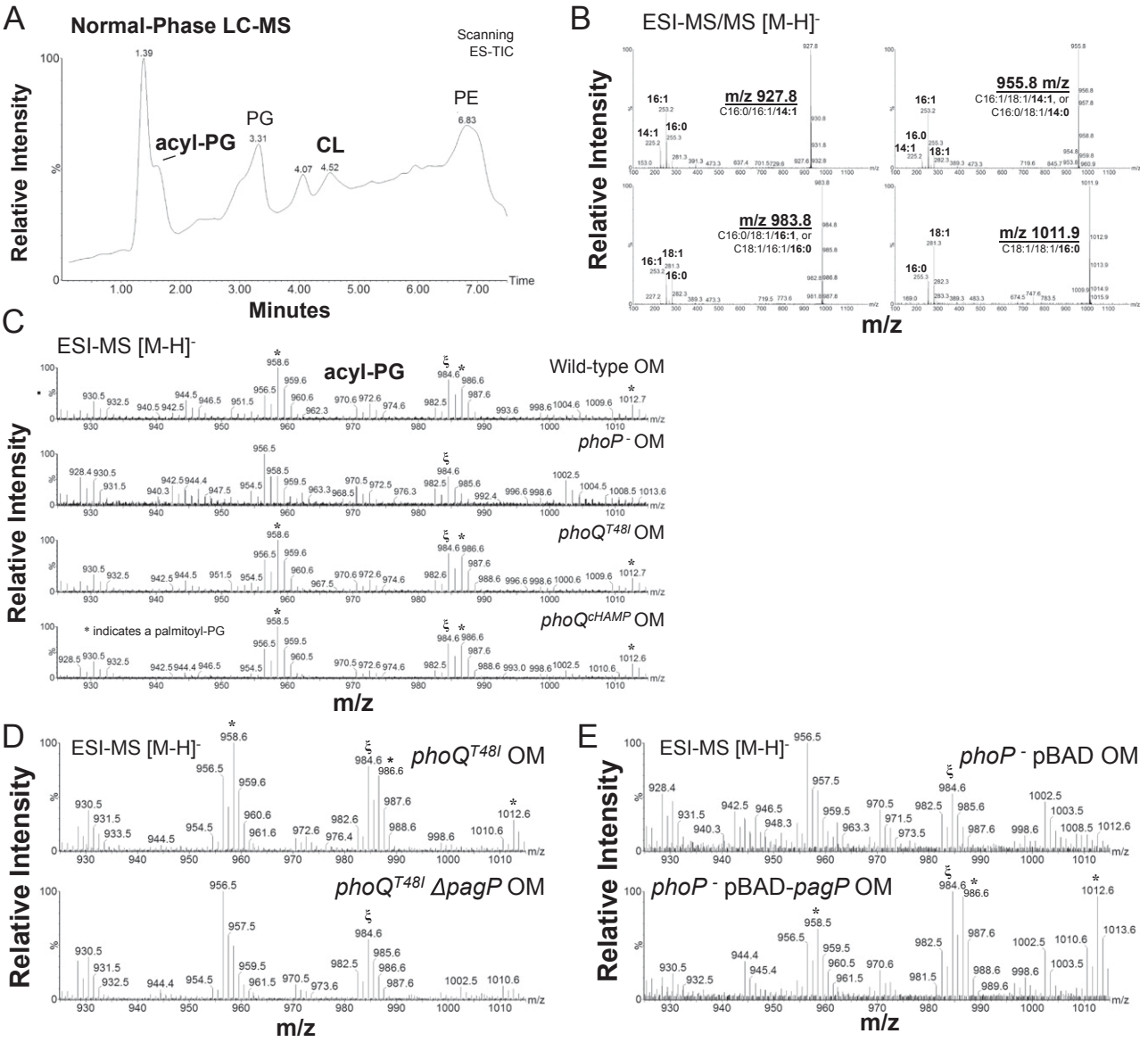


**Fig. S5.** (*A*) Depicted is the TIC chromatogram from normal-phase LC-MS/MS analysis of OM GPL. The retention times of the GPL were confirmed using commercial mixed-acyl standards. (*B*) Tandem quadrupole electrospray ionization collision induced dissociation (ESI-MS/MS) negative product-ion $[M\text{-}H]^-$ spectra of four acyl-PG species *m/z* 1012, 983, 955, and 927. (*C*) OM GPL were analyzed by ESI-TOF-MS in $[M\text{-}H]^-$ mode, and parent ions corresponding to acyl-PG were scanned for differences in relative abundance. Shown are extracts collected for one of four independent experiments. *Indicates an acyl-PG ion with palmitate (C16:0) at *sn-3′* (2). $^{\xi}$*m/z* 984.6 is the mass-to-charge ratio for two structurally distinct acyl-PG molecules: C16:0/18:1/16:0 and C16:0/18:1/16:1. MRM, multiple reaction monitoring. (*D*) ESI-MS from PhoPQ-activated bacteria with or without an intact *pagP* locus. *Indicates a *pagP*-regulated P-PG. (*E*) ESI-MS from *phoP* mutants overexpressing *pagP* from pBAD *in trans*.

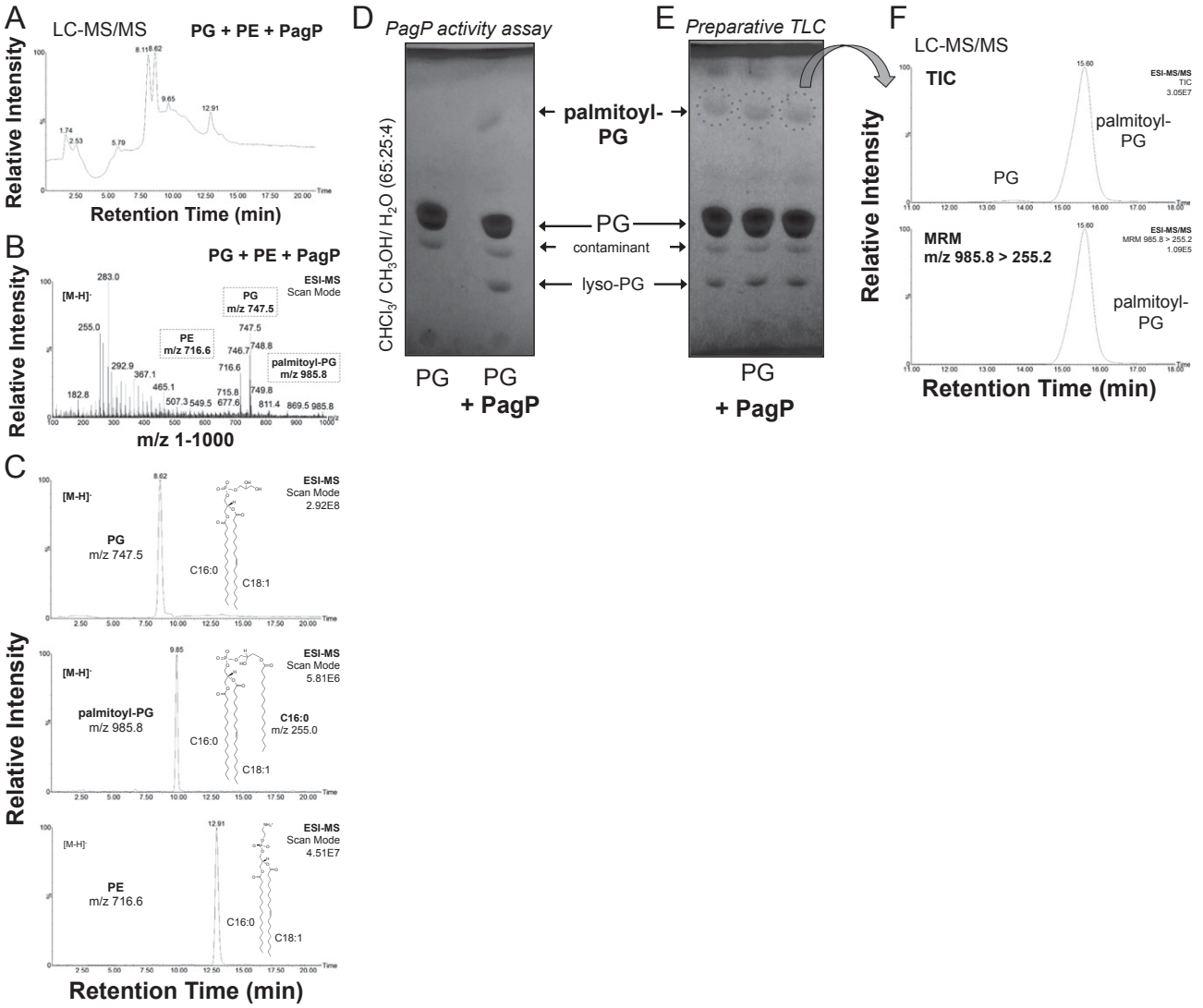


**Fig. S6.** To verify that the PagP-PG product was palmitoyl-PG, unlabeled PG and PE substrates were incubated with the PagP enzyme, and products were analyzed by LC-MS parent ion scanning. (*A*) PagP was incubated with a mixture of PE and PG, and resulting GPL were separated by LC to produce the TIC chromatogram shown. (*B*) Parent ion spectra from material eluting between 5 and 15 min were scanned. The predicted *m/z* of the palmitoyl-PG is *m/z* 985 (C16:0/C18:1/C16:0). (*C*) Using *m/z* values from parent ion analysis, the retention times of specific PG, PE, and palmitoyl-PG species were deduced. (*D*) To confirm that the faster migrating spot from the radiolabeled enzymatic reactions was palmitoyl-PG *m/z* 985.8 (C16:0/C18:1/C16:0), preparative TLC (*E*) and targeted LC-MS/MS (*F*) were performed. Iodine-stained silica containing the candidate palmitoyl-PG spot was combined, extracted, and targeted by LC-MS/MS and parent > daughter ion transition monitoring for the specific PG reactant and the predicted palmitoyl-PG product, *m/z* 985.8.

**Table S1. Bacterial strains and plasmids**

| Strain or plasmid | Genotype/phenotype | Source |
|---|---|---|
| *S.* Typhimurium | | |
| ATCC 14028s | Wild type | ATCC |
| CS015 | *phoP102*::Tn*10*d-cam (PhoP-null) | Miller lab collection |
| CS022 | $phoQ^{T48I}$, *a.k.a pho-24* (PhoPQ-activated) | Miller lab collection |
| CS330 | $phoQ^{T48I}$ *pagP1*::Tn*phoA* (PhoPQ-activated, PagP-null) | Miller lab collection |
| MB101 | *ΔphoQ*::Tn10d::*tet phoN105*::Tn*phoA* | Miller lab collection |
| LG062 | *pagP2*::Tn*10d-tet* | Miller lab collection |
| Plasmids | | |
| pBAD-*empty* | pBAD24 expression vector | (1) |
| pBAD-$phoQ^{WT}$ | pBAD24-*phoQ* wild type | Miller lab collection |
| pBAD-$phoQ^{T48I}$ | pBAD24-$phoQ^{T48I}$ classic *pho24* alllele | Miller lab collection |
| pBAD-$phoQ^{cHAMP}$ | pBAD24-$phoQ^{E232K}$ HAMP constitutive mutant | This study |
| pBAD-*pagP* | pBAD24-*pagP* vector for *pagP* overexpression | Miller lab collection |

1. Guzman LM, Belin D, Carson MJ, Beckwith J (1995) Tight regulation, modulation, and high-level expression by vectors containing the arabinose PBAD promoter. *J Bacteriol* 177(14): 4121–4130.

**Table S2. PhoPQ activation increases CL levels within the *S.* Typhimurium OM**

| GPL species $[M-H]^-$ | CL (pg)/PE (ng) in OM lipid extracts | | | |
|---|---|---|---|---|
| 1404 *m/z* CL (C68:3) | WT | *phoP* (1.1 ± 0.1) | *phoQT48I* (1.7 ± 0.4) | *phoQcHAMP* (3.5 ± 1.3) |
| 660 *m/z* PE C14:0/C16:1 | 61 ± 22 | 72 ± 24 | 136 ± 52 | 303 ± 125$^{*,\Psi}$ |
| 716 *m/z* PE C16:0/C18:1 | 33 ± 11 | 31 ± 7 | 49 ± 17 | 89 ± 29* |
| 742 *m/z* PE C18:1/C18:1 | 12 ± 4 | 13 ± 2 | 18 ± 10 | 35 ± 12$^{*,\Psi}$ |
| 1374 *m/z* CL (C66:3) | WT | *phoP* (1.3 ± 0.2) | *phoQT48I* (1.9 ± 0.5) | *phoQcHAMP* (4.4 ± 1.6) |
| 660 *m/z* PE C14:0/C16:1 | 87 ± 28 | 132 ± 45 | 214 ± 69* | 511 ± 191$^{*,\Psi}$ |
| 716 *m/z* PE C16:0/C18:1 | 48 ± 17 | 56 ± 15 | 77 ± 20* | 150 ± 42$^{*,\Psi}$ |
| 742 *m/z* PE C18:1/C18:1 | 17 ± 4 | 23 ± 5 | 29 ± 16 | 59 ± 18* |
| 1348 *m/z* CL (C64:2) | WT | *phoP* (1.1 ± 0.2) | *phoQT48I* (2.2 ± 0.5) | *phoQcHAMP* (4.5 ± 1.6) |
| 660 *m/z* PE C14:0/C16:1 | 51 ± 15 | 65 ± 25 | 144 ± 57* | 323 ± 127$^{*,\Psi}$ |
| 716 *m/z* PE C16:0/C18:1 | 29 ± 11 | 28 ± 8 | 51 ± 17* | 95 ± 28* |
| 742 *m/z* PE C18:1/C18:1 | 10 ± 3 | 12 ± 3 | 20 ± 11 | 37 ± 12* |
| 1322 *m/z* CL (C62:1) | WT | *phoP* (1.0 ± 0.1) | *phoQT48I* (1.9 ± 0.6) | *phoQcHAMP* (5.0 ± 1.9) |
| 660 *m/z* PE C14:0/C16:1 | 8 ± 3 | 9 ± 4 | 20 ± 13 | 56 ± 21$^{*,\Psi}$ |
| 716 *m/z* PE C16:0/C18:1 | 4 ± 2 | 4 ± 2 | 7 ± 5 | 16 ± 5$^{*,\Psi}$ |
| 742 *m/z* PE C18:1/C18:1 | 2 ± 1 | 2 ± 1 | 2 ± 1 | 6 ± 2$^{*,\Psi}$ |

Quantitative normal-phase LC-MS/MS determined the amount of CL species within the *S.* Typhimurium OM. Molecular formulas were derived from *E. coli* CL (1). The three PE species have distinct *m/z* values, which greatly diminishes signal contamination from unrelated chromatographically similar species with identical *m/z* values, as is the case for many GPL (3). Concentrations were measured using curves from commercial standards. Shown is the average ± SD from four experiments. Numbers in parentheses reflect the average fold difference ± SD for *mutant vs. WT* for all PE comparisons for that CL. *Value statistically different from WT ($P < 0.05$) by an unpaired two-tailed Student *t* test. $^{\Psi}$Value statistically different from $phoQ^{T48I}$ ($P < 0.05$). C, number of carbons atoms in a given acyl side chain, or for CL the total number of carbons in the molecule; CL, cardiolipin; GPL, glycerophospholipid; OM, outer membrane; PE, phosphatidylethanolamine. The number following the colon indicates the saturation state of the side chain, or molecule.

**Table S3. PhoPQ promotes the levels of acyl-PG molecules within the OM**

| GPL species $[M-H]^-$ | acyl-PG (pg)/PE (ng) in OM lipid extracts | | |
|---|---|---|---|
| 1012 *m/z* APG C18:1/18:1/16:0 | WT | *phoP* (−8.9 ± 1.4), (−14.8 ± 3.3$^{\omega}$) | *phoQT48I* (1.6 ± 0.1) |
| 660 *m/z* PE C14:0/C16:1 | 423 ± 139 | 46 ± 21$^{*,\Psi}$ | 882 ± 248* |
| 716 *m/z* PE C16:0/C18:1 | 143 ± 33 | 13 ± 5$^{*,\Psi}$ | 232 ± 102 |
| 742 *m/z* PE C18:1/C18:1 | 193 ± 58 | 23 ± 6$^{*,\Psi}$ | 296 ± 57* |
| 984 *m/z* APG C16:0/18:1/16:0, C16:0/18:1/16:1 | WT | *phoP* (−6.3 ± 0.9), (−8.6 ± 1.6$^{\omega}$) | *phoQT48I* (1.3 ± 0.2) |
| 660 *m/z* PE C14:0/16:1 | 1754 ± 907 | 268 ± 155$^{*,\Psi}$ | 2745 ± 1204 |
| 716 *m/z* PE C16:0/18:1 | 545 ± 315 | 76 ± 36$^{*,\Psi}$ | 645 ± 175 |
| 742 *m/z* PE C18:1/18:1 | 741 ± 475 | 137 ± 61$^{\Psi}$ | 970 ± 495 |
| 956 *m/z* APG C16:1/18:1/14:1, C16:0/18:1/14:0 | WT | *phoP* (−2.4 ± 0.3), (−4.4 ± 0.8$^{\omega}$) | *phoQT48I* (1.9 ± 0.3) |
| 660 *m/z* PE C14:0/16:1 | 1411 ± 608 | 578 ± 373$^{*,\Psi}$ | 3052 ± 1755 |
| 716 *m/z* PE C16:0/18:1 | 437 ± 214 | 164 ± 90$^{*,\Psi}$ | 696 ± 314 |
| 742 *m/z* PE C18:1/18:1 | 592 ± 330 | 298 ± 61* | 1084 ± 661 |
| 930 *m/z* APG C16:0/16:1/14:0 | WT | *phoP* (−2.7 ± 0.4), (−2.9 ± 0.6$^{\omega}$) | *phoQT48I* (1.1 ± 0.1) |
| 660 *m/z* PE C14:0/16:1 | 512 ± 136 | 186 ± 92$^{*,\Psi}$ | 646 ± 341 |
| 716 *m/z* PE C16:0/18:1 | 159 ± 53 | 53 ± 20* | 159 ± 79 |
| 742 *m/z* PE C18:1/18:1 | 213 ± 85 | 95 ± 29$^{*,\Psi}$ | 222 ± 99 |

Quantitative reversed-phase LC-MS/MS was used to measure the amount of APG/PE (pg/ng) in lipid extracts collected from OM fractions. *Denotes an average pg/ng value statistically different from WT ($P < 0.05$) by an unpaired, two-tailed Student *t* test. $^{\Psi}$Indicates a *phoP* mutant extract statistically different from *phoQ*$^{T48I}$ ($P < 0.05$). Numbers in parentheses reflect the average fold difference ± SD *mutant vs. WT* of all three PE comparisons for that APG. $^{\omega}$Denotes the average fold difference ± SD in *phoP* vs. *phoQ*$^{T48I}$. Acyl substituents were defined by collision-induced dissociation (CID) fragmentation analysis (Fig. S6) and structural characterizations described previously for *E. coli* (3) and *S.* Typhimurium GPL (2). APG, acyl-phosphatidylglyerol. As for Table S2, three PE species were chosen for analysis. Exact concentrations were determined using standard curves and commercial standards. Shown is the average amount of APG/ PE ± SD from three independent experiments.

**Table S4. PagP is required for increases in OM palmitoyl-PG on PhoPQ activation**

| GPL species $[M-H]^-$ | acyl-PG (ng)/PE (ng) in OM lipid extracts | |
|---|---|---|
| 1012 *m/z* APG C18:1/18:1/16:0 | *phoQT48I* | *phoQT48I pagP* (−13.7 ± 2.4) |
| 660 *m/z* PE C14:0/C16:1 | 492 ± 253 | 36 ± 5* |
| 716 *m/z* PE C16:0/C18:1 | 68 ± 27 | 4 ± 3* |
| 742 *m/z* PE C18:1/C18:1 | 123 ± 43 | 11 ± 7* |
| 958 *m/z* APG C16:0/16:1/16:0, C16:0/18:1/14:0 | *phoQT48I* | *phoQT48I pagP* (−13.9 ± 3.4) |
| 660 *m/z* PE C14:0/C16:1 | 2115 ± 726 | 168 ± 67* |
| 716 *m/z* PE C16:0/18:1 | 314 ± 100 | 18 ± 10* |
| 742 *m/z* PE C18:1/18:1 | 607 ± 162 | 53 ± 31* |
| 956 *m/z* APG C16:1/18:1/14:1, C16:0/18:1/14:0 | *phoQT48I* | *phoQT48I pagP* (−2.2 ± 0.5) |
| 660 *m/z* PE C14:0/C16:1 | 3844 ± 1085 | 2045 ± 790* |
| 716 *m/z* PE C16:0/18:1 | 587 ± 238 | 217 ± 116* |
| 742 *m/z* PE C18:1/18:1 | 1150 ± 24 | 642 ± 367* |
| 930 *m/z* APG C16:0/16:1/14:0 | *phoQT48I* | *phoQT48I pagP* (−2.5 ± 0.6) |
| 660 *m/z* PE C14:0/C16:1 | 647 ± 251 | 289 ± 144* |
| 716 *m/z* PE C16:0/18:1 | 102 ± 62 | 32 ± 21 |
| 742 *m/z* PE C18:1/18:1 | 204 ± 127 | 96 ± 67 |

Quantitative reversed-phase LC-MS/MS determined the amount of APG/ PE (pg/ng) in lipid extracts collected from OM fractions. *Denotes an average value statistically different from *phoQ*$^{T48I}$ ($P < 0.05$) by an unpaired, two-tailed Student *t* test. Numbers in parentheses reflect the average fold difference ± SD *phoQ*$^{T48I}$ *pagP vs. phoQ*$^{T48I}$ of all three PE comparisons for that APG. Exact concentrations were determined using standard curves and commercial standards. Shown is the average amount of APG/ PE ± SD from three independent experiments.

**Table S5. PagP is sufficient for OM palmitoyl-PG formation in *phoP* mutants**

| GPL species $[M-H]^-$ | acyl-PG (ng)/PE (ng) in OM lipid extracts | |
|---|---|---|
| 1012 *m/z* APG C18:1/18:1/16:0 | *phoP* pBAD | *phoP* pBAD-*pagP* (11.0 ± 9.1) |
| 716 *m/z* PE C16:0/C18:1 | 19 ± 6 | 326 ± 99* |
| 742 *m/z* PE C18:1/C18:1 | 34 ± 11 | 156 ± 11* |
| 958 *m/z* APG C16:0/16:1/16:0, C16:0/18:1/14:0 | *phoP* pBAD | *phoP* pBAD-*pagP* (5.8 ± 4.4) |
| 716 *m/z* PE C16:0/18:1 | 64 ± 22 | 586 ± 216 |
| 742 *m/z* PE C18:1/18:1 | 118 ± 43 | 311 ± 222 |
| 956 *m/z* APG C16:1/18:1/14:1, C16:0/18:1/14:0 | *phoP* pBAD | *phoP* pBAD-*pagP* (2.2 ± 1.7) |
| 716 *m/z* PE C16:0/18:1 | 248 ± 68 | 834 ± 306 |
| 742 *m/z* PE C18:1/18:1 | 459 ± 144 | 436 ± 244 |
| 930 *m/z* APG C16:0/16:1/14:0 | *phoP* pBAD | *phoP* pBAD-*pagP* (2.9 ± 2.1) |
| 716 *m/z* PE C16:0/18:1 | 32 ± 11 | 139 ± 82 |
| 742 *m/z* PE C18:1/18:1 | 59 ± 23 | 80 ± 73 |

Quantitative reversed-phase LC-MS/MS determined the amount of APG/ PE (pg/ng) in lipid extracts collected from OM fractions. *Denotes an average value statistically different from *phoP* ($P < 0.05$) by an unpaired, two-tailed Student *t* test. Numbers in parentheses reflect the average fold difference ± SD *phoP* pBAD-*pagP vs. phoP* pBAD of both PE comparisons for that APG. Note: PagP overexpression reduced levels of some PE species including *m/z* 660, likely due to its phospholipase activity, which is why this PE is excluded. Exact concentrations were determined using standard curves and commercial standards. Shown is the average amount of APG/ PE ± SD from three independent experiments.